

ChemComm

Accepted Manuscript



This is an *Accepted Manuscript*, which has been through the Royal Society of Chemistry peer review process and has been accepted for publication.

Accepted Manuscripts are published online shortly after acceptance, before technical editing, formatting and proof reading. Using this free service, authors can make their results available to the community, in citable form, before we publish the edited article. We will replace this *Accepted Manuscript* with the edited and formatted *Advance Article* as soon as it is available.

You can find more information about *Accepted Manuscripts* in the [Information for Authors](#).

Please note that technical editing may introduce minor changes to the text and/or graphics, which may alter content. The journal's standard [Terms & Conditions](#) and the [Ethical guidelines](#) still apply. In no event shall the Royal Society of Chemistry be held responsible for any errors or omissions in this *Accepted Manuscript* or any consequences arising from the use of any information it contains.

Cite this: DOI: 10.1039/c0xx00000x

www.rsc.org/xxxxxx

COMMUNICATION

Single functionalized graphene oxide reconstitutes kinesin mediated intracellular cargo transport, delivers multiple cytoskeleton proteins and therapeutic molecule into the cell

Batakrishna Jana, Atanu Biswas, Saswat Mohapatra, Abhijit Saha and Surajit Ghosh*

Received (in XXX, XXX) Xth XXXXXXXXXX 20XX, Accepted Xth XXXXXXXXXX 20XX

DOI: 10.1039/b000000x

Here, we report a covalently functionalized graphene oxide with Tris-(nitrilo Tris-acetic acid) (TGO), which can reconstitute kinesin mediated intracellular cargo transport, delivers multiple proteins and therapeutic antimetabolic dodecapeptide peptide into the cancer cell.

Chemically functionalized nano-/micro-graphene oxide and its composites have huge implications on the development of biomedical and biotechnological devices because of their excellent thermal, mechanical, electrical and chemical properties.¹ GO can be covalently functionalized with biocompatible polymers such as polyethylene glycol (PEG) through reactive functionalities such as epoxy and hydroxyl group on the basal plane and carboxylic groups along the sheet edge for its stability in physiological environment.² PEGylated GO can be further modified through covalent chemical reaction using various small molecules such as Tris-(nitrilo Tris-acetic acid) (Tris-NTA), NTA, biotin, drugs etc. and through noncovalent surface coating with proteins, nucleic acids etc.³ Various research groups have recently demonstrated that GO composites have wide range of tissue engineering applications such as growth and differentiation of human mesenchymal and neuronal stem cells,⁴ detection of electrical changes in cell membrane,⁵ targeted drug or gene carriers,^{6a} cancer photothermal therapy,^{6b} specific cell labelling^{6a} and *in vivo* tumor positron emission tomography (PET) imaging.^{6c} Recently, we and other groups have demonstrated by *in vitro* and *in vivo* experiments that functionalized graphene oxides are nontoxic to cells^{4, 7b} and mice.⁸ We have shown previously that Tris-NTA and biotin functionalized GO can deliver both oligo-histidine and biotin tagged proteins simultaneously into the cell.^{7b} In this report, we demonstrate that Tris-NTA functionalized Graphene Oxide (TGO) is capable of doing multiple tasks such as walking along the microtubule with a cargo protein, carries multiple cytoskeleton proteins and therapeutic microtubule targeted peptide into the cell.

Synthesis of TGO (Scheme S1)⁷ and its' characterization by UV/Vis and FT-IR spectroscopic method (Fig. S2) were described in supplementary section. Surface morphology was studied by Atomic Force Microscopy (AFM), Transmission Electron Microscopy (TEM) and High Resolution Transmission Electron Microscopy (HR-TEM). AFM, TEM and HR-TEM

images reveal the significant changes in surface height, morphology and pattern after functionalization (Fig. S3-S6). Detailed is in supplementary section. We have also characterized the average size of TGO nanoparticle by Dynamic Light Scattering (DLS) measurements, which indicated that the average particle size of the TGO is 213 nm with PDI-0.384 (Fig. S7).

Spatial organization of the cytoskeleton and intracellular transport of various cargoes such as cellular organelles and small vesicles are maintained by cytoskeletal molecular motor proteins.⁹ They are mechanochemical enzymes, which can walk

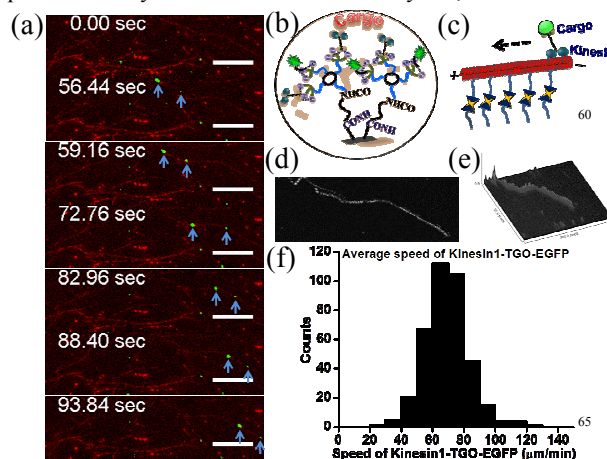


Fig. 1 (a) Time lapse images indicating the positions of Kinesin1-TGO-EGFP nanoparticles conjugate on surface immobilized microtubules with time. (b) Cartoon diagram of the Kinesin1-TGO-EGFP conjugate. (c) Cartoon representation of transport of Kinesin1-TGO-EGFP nanoparticle conjugates on microtubule. (d) Z-projection 2D image shows the steps of Kinesin1-TGO-EGFP walk along the microtubules. (e) 3D footage of the transport of Kinesin1-TGO-EGFP nanoparticles onto the microtubule lattice. (f) Histogram shows the speed of the Kinesin1-TGO-EGFP nanoparticles. Scale bar corresponds to 10 μm.

on the microtubules. There are two classes of microtubule motor proteins. One is kinesin and another one is dynein. Kinesin1 is the most extensive studied molecular motor protein, which moves processively towards the plus-end of microtubule using adenosine triphosphate (ATP) as energy source. Purified Kinesin1 is either used for *in vitro* microtubule gliding assay or for the transport of beads, CNT and vesicles along the immobilized microtubules onto the surface.¹⁰ However, transport of graphene oxide has not

yet been reported. Here, we have shown the long range transport of Kinesin1-TGO-EGFP along the various microtubules in a well-controlled manner. EGFP-His₁₀ and Kinesin612-His₁₀ were loaded onto the Ni²⁺-TGO at physiological condition following the method, described in the supplementary section. Next, flow chamber was prepared with biotinylated glass and biotinylated Alexa568 labeled taxol stabilized microtubules were immobilized followed by equilibration of flow chamber with motility buffer containing ATP. Finally, EGFP-His₁₀ and kinesin612-His₁₀ loaded Ni²⁺-TGO in motility buffer was loaded to the flow chamber and time lapse images were recorded in the TIRF microscope at 488 and 561 nm channel simultaneously (ESI). Time lapse images from transport movie reveals that Kinesin1-TGO-EGFP is excellently walking along the microtubules as soon as they land onto the microtubules lattice (Fig. 1a, MovieS1) as we observed that the green colored nanoparticles are walking along the red colored microtubules. Fig. 1a represents the time lapse images from a movie and cyan arrows indicate the position of the Kinesin1-TGO-EGFP nanoparticles onto the microtubule lattice changes with progress of time. Fig. 1b and Fig. 1c represent the cartoon diagram of Kinesin1-TGO-EGFP nanoparticle conjugate and transport of the conjugate on microtubule respectively. We have observed 2D and 3D footage of Kinesin1-TGO-EGFP nanoparticles transport onto the microtubule lattice (Fig. 1d and Fig. 1e). We have also calculated the average transport velocity of the Kinesin1-TGO-EGFP nanoparticles from multiple movies and found that the average transport velocity is $68.83 \pm 14.14 \mu\text{m}/\text{min}$ (Fig. 1f), which indicates that the transportation of TGO is most likely guided by single kinesin as well as multiple kinesin. This result clearly indicates that TGO is capable of capture two proteins and among them one is functional proteins, which has huge potential in biotechnological applications.

Next, we have tried to load five proteins through primary and secondary interactions with Ni-TGO surface in physiological condition. Among five proteins we have chosen four proteins from cytoskeleton proteins as we found kinesin is active and transport TGO. The schematic view of proteins binding with TGO is shown in Fig. 2a. In brief, cytoskeleton proteins were loaded onto the TGO following the method described in supplementary section and characterized by DLS (Fig. S8) and TEM (Fig. S9) followed by imaging under fluorescence microscope. Fluorescence microscopic images reveal that the co-existence of green color nanoparticles in 488 nm channel (Fig. 2b) and red color nanoparticles in 561 nm (Fig. 2c) and 638 nm channel (Fig. 2d). Fig. S10 represents the DIC image of multiple proteins loaded TGO. Green fluorescence comes from microtubule end binding protein Mal3-EGFP. Mal3-EGFP is attached to TGO through V_HH-His₆ antibody, which selectively captures GFP protein.¹¹ Red fluorescence at 561 nm comes from mCherry labeled microtubule minus-end directed microtubule cross linking motor (Xenopus kinesin-14 XCTK2 with hexa His tag) mCherry-XCTK2-His₆,^{12a} which is directly attached with TGO. Another red fluorescence at 638 nm comes from Cy5-labeled tubulin, which is bound with immobilized microtubule polymerase XMAP215-His₇ (a *Xenopus laevis* chTOG family member)^{12b} onto TGO. Therefore, above result clearly indicates that TGO has the capability of binding with multiple cytoskeleton

proteins simultaneously through primary and secondary interactions. We have performed control experiment with PEGylated GO following same procedure to check whether this

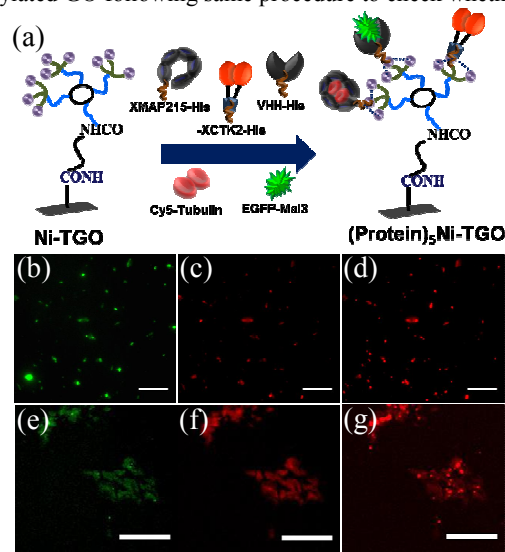


Fig. 2 (a) Cartoon diagram of multiple cytoskeleton proteins loaded TGO. Fluorescence microscopic images in (b) 488 nm, (c) 561 nm and (d) 638 nm channel clearly indicate the loading of microtubule end binding protein Mal3-EGFP through V_HH-His₆ antibody, mCherry-XCTK2-His₆ and Cy5-labeled tubulin through microtubule polymerase XMAP215-His₇ respectively on TGO. Scale bar corresponds to 10 μm . Cellular uptake of multiple cytoskeleton proteins loaded TGO in A549 cell line. Images at (e) 488 nm, (f) 561 nm and (g) 638 nm channel indicate uptake of multiple cytoskeleton proteins loaded TGO by A549 cells. Scale bar corresponds to 100 μm .

binding is through Tris-NTA functionalization or nonspecific. Absence of significant fluorescence signals at 488, 561 and 638 nm channel indicates that the binding was occurred only through Tris-NTA functionalization (Fig. S11). Further, we have studied whether TGO is capable of delivering multiple proteins into the cell or not. Initially, we have checked the cytotoxicity of the TGO nanoparticles by the MTT assay in human lung cancer cell line (A549) and human breast cancer cell line (MCF-7) and found non-cytotoxic nature of TGO particles (Fig. S12). Subsequently, the cellular uptake of multiple cytoskeleton proteins loaded TGO nanoparticles was studied in A549 and MCF-7 cell line. Multiple cytoskeleton proteins were loaded to the TGO following similar method as described in the supplementary section and cellular uptake has been achieved with this multiple cytoskeleton proteins loaded TGO. From the fluorescence images, it was found that green signals in 488 nm channel (Fig. 2e and Fig. S13c) and red signals in 561 (Fig. 2f and Fig. S13b) and 638 nm channels (Fig. 2g and Fig. S13d) inside both A549 and MCF-7 cells, which confirms the uptake of all five proteins (V_HH-His₆, mCherry-XCTK2-His₆, XMAP215-His₇, Mal3-EGFP and Cy5-tubulin) loaded TGO.

Finally, we have studied the therapeutic application of TGO. For that purpose we have decided to use microtubule targeted peptide (FRRKAFLHWYMTG) which is known to inhibit tubulin polymerization and cell proliferation at approximately 180 μM concentration.¹³ This biotinylated dodecapeptide was synthesized (Fig. S14) and attached with TGO (dodecapeptide-

TGO) through streptavidin biotin interaction, as we have attached Streptavidin-His₆ with Ni²⁺-TGO prior to peptide attachment. Now, we have checked the anti-cancer efficacy of the dodecapep-

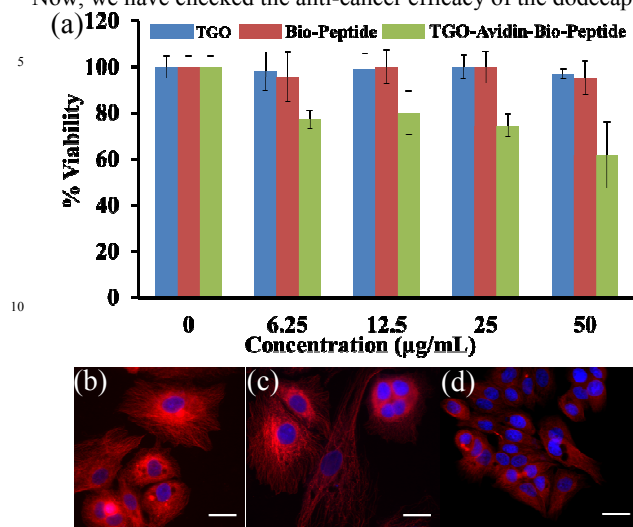


Fig. 3 (a) Survival of MCF-7 cell line was assessed by MTT assay after treatment with TGO, biotinylated dodecapeptide, Dodecapeptide-TGO for 24 hours. Microtubules network of MCF-7 cell lines after treatment with (b) biotinylated dodecapeptide, (c) TGO and (d) Dodecapeptide-TGO conjugate. Scale bar corresponds to 30 µm.

-tide-TGO conjugate by MTT assay in MCF-7 cell line. Interestingly, it was found that the dodecapeptide-TGO is killing ~40% cancer cell at 50 µg/mL concentration while the TGO and bio-dodecapeptide peptide is non-cytotoxic in nature at similar concentration (Fig. 3a). This result clearly indicates that TGO acts as an excellent delivery vehicle for therapeutic molecules as the cancer cell killing efficacy of the dodecapeptide increases in presence of TGO. Since dodecapeptide-TGO conjugate is killing ~40% MCF-7 cells and the peptide is known to target tubulin polymerization, therefore, we became interested to study microtubule organization inside MCF-7 cells after dodecapeptide-TGO conjugate treatment. For that purpose the cells were treated with biotinylated dodecapeptide, TGO and dodecapeptide-TGO conjugate separately for 24 hours and microtubule network was visualized by sequential treatment of primary and secondary antibody (ESI) and observed under inverted fluorescence microscope (Model Nikon Eclipse Ti-U). From the microscopic images, it was observed that there was no effect of TGO (Fig. 3c and Fig. S16) and biotinylated dodecapeptide at 50 µg/mL concentration (Fig. 3b and Fig. S17) on microtubules network of MCF-7 cell lines as there was no difference of microtubules network between untreated (Fig. S15) and treated cells. But, we have observed that dodecapeptide-TGO conjugate disrupts the microtubule network of the MCF-7 cell line and as a result shrinking of cells occurred (Fig. 3d and Fig S18).

In conclusion, we have shown that non-cytotoxic TGO is capable to perform multiple tasks such as, walking along the microtubules, bind with multiple proteins simultaneously, deliver those proteins and microtubule targeted therapeutic molecules into the cell. To the best of our knowledge, this work is the first example for future development of graphene based hybrid nano-machine and currently, we are working on that direction.

Authors wish to thank CSIR-IICB network project (BSC0113)

and imaging facility (TIRF and Technai POLARA TEM), NCCS-Pune, Dr. T. Surrey, Cancer Research UK, Prof. K. Bhattacharyya (IACS, Kolkata), Prof. D. Chowdhury and Prof. S. Verma, IIT Kanpur, CSIR (to BJ and AS), UGC (to AB and SM) and DST (to SG for Ramanujan fellowship).

Notes and references

- ^a Chemistry Division, CSIR-Indian Institute of Chemical Biology, 4 Raja S. C. Mullick Road, Jadavpur, Kolkata-700032, West Bengal, India. Fax: +91-33-2473-5197/0284; Tel: +91-33-2499-5872; E-mail: sghosh@iicb.res.in
- † Electronic Supplementary Information (ESI) available: See DOI: 10.1039/b000000x/
- (a) K. Yang, L. Feng, X. Shi and Z. Liu, *Chem. Soc. Rev.*, 2013, **42**, 530; (b) D. Bitounis, H. Ali-Boucetta, B. H. Hong, D. H. Min and K. Kostarelos, *Adv. Mater.*, 2013, **25**, 2258; (c) H. Shen, L. Zhang, M. Liu and Z. Zhang, *Theranostics*, 2012, **2**, 283; (d) Y. Zhang, T. R. Nayak, H. Hong and W. Cai, *Nanoscale*, 2012, **4**, 3833; (e) C. N. R. Rao, A. K. Sood, K. S. Subrahmanyam and A. Govindaraj, *Angew. Chem. Int. Ed.*, 2009, **48**, 7752.
 - (a) K. Yang, S. Zhang, G. Zhang, X. Sun, S. T. Lee and Z. Liu, *Nano Lett.*, 2010, **10**, 3318; (b) S. A. Zhang, K. Yang, L. Z. Feng and Z. Liu, *Carbon*, 2011, **49**, 4040.
 - (a) J. H. Jung, D. S. Cheon, F. Liu, K. B. Lee and T. S. Seo, *Angew. Chem. Int. Ed.*, 2010, **49**, 5708; (b) C. H. Lu, H. H. Yang, C. L. Zhu, X. Chen and G. N. Chen, *Angew. Chem. Int. Ed.*, 2009, **48**, 4785; (c) L. Zhang, Z. Lu, Q. Zhao, J. Huang, H. Shen and Z. Zhang, *Small*, 2011, **7**, 460; (d) Y. Guo, S. Guo, J. Ren, Y. Zhai, S. Dong and E. Wang, *ACS Nano*, 2010, **4**, 4001; (e) J. T. Robinson, S. M. Tabaknam, Y. Liang, H. Wang, H. S. Casalongue, D. Vinh and H. Dai, *J. Am. Chem. Soc.*, 2011, **133**, 6825.
 - (a) W. C. Lee, C. H. Y. X. Lim, H. Shi, L. A. L. Tang, Y. Wang, C. T. Lim and K. P. Loh, *ACS Nano*, 2011, **5**, 7334; (b) T. R. Nayak, H. Andersen, V. S. Makam, C. Khaw, S. Bae, X. Xu, P. L. R. Ee, J. H. Ahn, B. H. Hong, G. Pastorin and B. Özyilmaz, *ACS Nano*, 2011, **5**, 4670; (c) A. Bianco, *Angew. Chem. Int. Ed.*, 2013, **52**, 4986.
 - T. Cohen-Karni, Q. Qing, Q. Li, Y. Fang and C. M. Lieber, *Nano Lett.*, 2010, **10**, 1098.
 - (a) W. Zhang, Z. Guo, D. Huang, Z. Liu, X. Guo and H. Zhong, *Biomaterials*, 2011, **32**, 8555; (b) K. Yang, L. Hu, X. Ma, S. Ye, L. Cheng, X. Shi, C. Li, Y. Li and Z. Liu, *Adv. Mater.*, 2012, **24**, 1868; (c) H. Hong, K. Yang, Y. Zhang, J. W. Engle, L. Feng, Y. Yang, T. R. Nayak, S. Goel, J. Bean, C. P. Theuer, T. E. Barnhart, Z. Liu and W. Cai, *ACS Nano*, 2012, **6**, 2361.
 - (a) W. S. Hummers and R. E. Offeman, *J. Am. Chem. Soc.*, 1958, **80**, 1339; (b) B. Jana, G. Mondal, A. Biswas, I. Chakraborty, A. Saha, P. Kurkute and S. Ghosh, *Macromol. Biosci.*, 2013, **13**, 1478.
 - (a) Y. Li, Y. Liu, Y. Fu, T. Wei, L. Le Guyader, G. Gao, R. S. Liu, Y. Z. Chang and C. Chen, *Biomaterials*, 2012, **33**, 402; (b) K. Yang, H. Gong, X. Shi, J. Wan, Y. Zhang and Z. Liu, *Biomaterials*, 2013, **34**, 2787.
 - (a) H. Miki, Y. Okada and N. Hirokawa, *Trends Cell Biol.*, 2005, **15**, 467; (b) R. Mallik and S. P. Gross, *Curr. Biol.*, 2004, **14**, R971.
 - (a) R. K. Doot, H. Hess and V. Vogel, *Soft Matter*, 2006, **3**, 349; (b) Y. Jeune-Smith, A. Agarwal and H. Hess, *J. Vis. Exp.*, 2010, **45**; (c) M. Bhagawati, S. Ghosh, A. Reichel, K. Froehner, T. Surrey and J. Piehler, *Angew. Chem. Int. Ed.*, 2009, **48**, 9188; (d) C. Herold, C. Leduc, R. Stock, S. Diez and P. Schwill, *ChemPhysChem*, 2012, **13**, 1001; (e) J. Beeg, S. Klumpp, R. Dimova, R. S. Graci, E. Unger and R. Lipowsky, *Biophys. J.*, 2008, **94**, 532; (f) K. Bçhm, R. Stracke, P. Mhlig and E. Unger, *Nanotechnology*, 2001, **12**, 238.
 - (a) S. P. Maurer, P. Bieling, J. Cope, A. Hoenger and T. Surrey, *Proc. Natl. Acad. Sci. U.S.A.*, 2011, **108**, 3988; (b) A. Biswas, A. Saha, D. Ghosh, B. Jana and S. Ghosh, *Soft Matter*, 2014, **10**, 2341.
 - (a) C. Hentrich and T. Surrey, *J. Cell Biol.*, 2010, **189**, 465. (b) G. J. Brouhard, J. H. Stear, T. L. Noetzel, J. Al-Bassam, K. Kinoshita, S. C. Harrison, J. Howard and A. A. Hyman, *Cell*, 2008, **132**, 79.
 - S. Pieraccini, G. Saladino, G. Cappelletti, D. Cartelli, P. Francescato, G. Speranza, P. Manitto and M. Sironi, *Nat Chem.*, 2009, **1**, 642.